

# T<sub>1</sub>, T<sub>2</sub> Relaxation and Magnetization Transfer in Tissue at 3T

Greg J. Stanisz,<sup>1,2\*</sup> Ewa E. Odobina,<sup>1</sup> Joseph Pun,<sup>1</sup> Michael Escaravage,<sup>1</sup> Simon J. Graham,<sup>1,2</sup> Michael J. Bronskill,<sup>1,2</sup> and R. Mark Henkelman,<sup>1,2,3</sup>

**T<sub>1</sub>, T<sub>2</sub>, and magnetization transfer (MT) measurements were performed in vitro at 3 T and 37°C on a variety of tissues: mouse liver, muscle, and heart; rat spinal cord and kidney; bovine optic nerve, cartilage, and white and gray matter; and human blood. The MR parameters were compared to those at 1.5 T. As expected, the T<sub>2</sub> relaxation time constants and quantitative MT parameters (MT exchange rate, R, macromolecular pool fraction, M<sub>0B</sub>, and macromolecular T<sub>2</sub> relaxation time, T<sub>2B</sub>) at 3 T were similar to those at 1.5 T. The T<sub>1</sub> relaxation time values, however, for all measured tissues increased significantly with field strength. Consequently, the phenomenological MT parameter, magnetization transfer ratio, MTR, was lower by approximately 2 to 10%. Collectively, these results provide a useful reference for optimization of pulse sequence parameters for MRI at 3 T. Magn Reson Med 54:507–512, 2005. © 2005 Wiley-Liss, Inc.**

**Key words:** 3 T; magnetization transfer; T<sub>1</sub>; T<sub>2</sub>; MTR; liver; cartilage; muscle; heart; spinal cord; kidney; white matter; gray matter; blood

Longitudinal, T<sub>1</sub>, and transverse, T<sub>2</sub>, relaxation time measurements are relevant in understanding water molecular dynamics in biologic systems. T<sub>1</sub>, T<sub>2</sub> relaxation times and MT depend on the chemical and physical environments of water protons in tissue. MRI contrast between normal and pathologic tissue is often based on differences in tissue microstructure and, therefore, different T<sub>1</sub> and T<sub>2</sub> relaxation times. Moreover, T<sub>1</sub>, T<sub>2</sub>, and MT provide quantitative assessment of tissue pathology. In particular, they offer additional information about the processes of demyelination and axonal loss (1–4), inflammation (5), infarction (6), white matter edema (7), tumor malignancy (8), and ischemia (9). Both tissue relaxation and MT parameter estimates are important in designing MRI pulse sequences that aim to accentuate contrast between normal and patho-

logic tissue. Since MRI at higher fields (particularly 3 T) has become more common, it is important to evaluate MR parameters of tissue quantitatively to determine MRI sequence parameters, such as TE (echo time), TR (repetition time), or MT saturation schemes, that provide an optimal contrast. The literature data regarding MR parameters at high fields (such as 3 T) is surprisingly limited. The goal of this study is to provide a comprehensive evaluation of MR parameters at 3 T to serve as reference for further MRI pulse sequence optimization. Therefore, T<sub>1</sub> and T<sub>2</sub> relaxation, and MT parameters at 3 T and 37°C for a wide range of tissues: liver, muscle, optic nerve, spinal cord, heart, kidney, white (corpus callosum) and gray matter (brain cortex), cartilage, and blood were measured and compared to those at 1.5 T.

## EXPERIMENTAL METHODS

### MR Measurements

All 3 T, MR measurements were performed at 37°C using a research-dedicated, whole body GE SIGNA magnet. MR pulse sequences and data acquisition were controlled by an NMR spectroscopy console (SMIS, Surrey, England). Rectangular radiofrequency (RF) pulses were transmitted by an RF amplifier (American Microwave Technology, Brea, CA; model 3205) and solenoid RF coil designed to accommodate in vitro tissue measurements in test tubes (9 turns, 8 mm in diameter, 15 mm length). Immediately after tissue excision, the samples (approximately 300 μL by volume) were immersed in non-protonated, MR-compatible fluid (Fluorinert; 3M, London, Canada) to avoid dehydration and reduce magnetic susceptibility effects. Temperature was controlled by an air-flow mechanism with MR-compatible thermocouple (Luxtron) inserted into the measured sample. The accuracy of sample temperature was approximately 0.5°. The measurements for a single sample lasted approximately 2 h. Before and after each experimental session, a multicomponent, T<sub>2</sub> decay was measured using a Carr–Purcell–Meiboom–Gill (CPMG) (10,11) sequence to confirm no degradation of the sample signal characteristics. The multi-component T<sub>2</sub> decay curves varied less than 1% during these sessions, indicating that the samples were stable over the time-course of the MR experiments. The MR parameters and biologic variations for each tissue were determined from independent measurements of 3 tissue samples. The T<sub>1</sub> and T<sub>2</sub> relaxation measurements were then repeated at 1.5 T (Nalorac, 1.5 T magnet) with identical MR pulse sequence param-

<sup>1</sup>Imaging Research, Sunnybrook & Women's College Health Sciences Centre, Toronto, ON, Canada.

<sup>2</sup>Department of Medical Biophysics, University of Toronto, Toronto, ON, Canada.

<sup>3</sup>Mouse Imaging Centre (MICe), Hospital for Sick Children, Toronto, ON, Canada.

Grant sponsor: Terry Fox Program, National Cancer Institute of Canada. Grant sponsor: Canadian Institutes for Health Research; Grant numbers: MT15598 and MOP57894.

\*Correspondence to: Greg J. Stanisz, PhD, Imaging Research, Sunnybrook & Women's College Health Sciences Centre, S655–2075 Bayview Avenue, Toronto, ON, Canada M4N 3M5. E-mail: stanisz@sten.sunnybrook.utoronto.ca Received 3 February 2005; revised 14 April 2005; revised 14 April 2005; accepted 18 April 2005.

DOI 10.1002/mrm.20605

Published online 5 August 2005 in Wiley InterScience (www.interscience.wiley.com).

© 2005 Wiley-Liss, Inc.

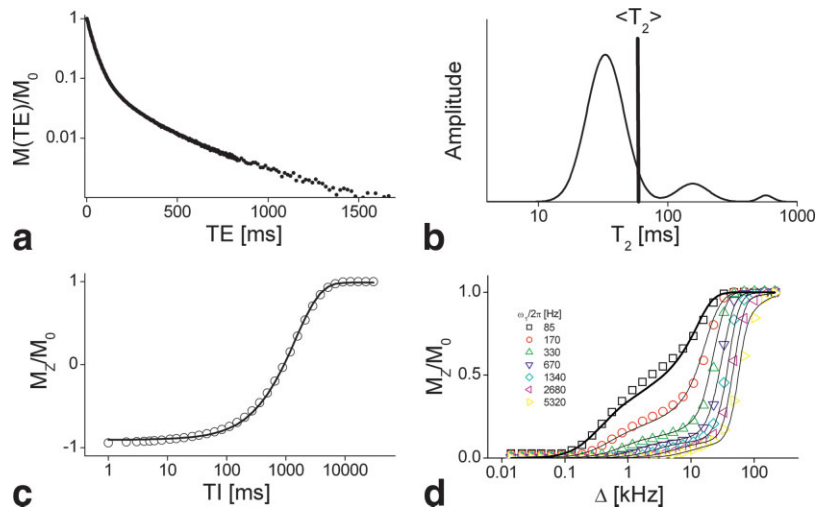


FIG. 1. (a)  $T_2$  decay in muscle tissue as measured by a CPMG sequence. For clarity, only 600 (out of 6000) data points are shown. The experimental data exhibits “upward” curvature, indicating non-monoexponential  $T_2$  behavior. Although it appears that only the first 1500 have a useful SNR, using all 6000 echoes for data analysis ensures NNLS fit stability and accuracy of determining long  $T_2$  relaxation times, and allows the estimation of SNR. (b) The  $T_2$  spectrum for the data shown in (a). The  $T_2$  spectrum is a result of an NNLS fit and shows as a function of  $T_2$  relaxation times the relative signal amplitude per logarithmic interval. In the case of muscle, 3 well distinguished  $T_2$  components are observed. The physical interpretation of the observed  $T_2$  peaks is beyond the scope of this study. As a single-parameter summary of the  $T_2$  spectrum, an average  $T_2$  relaxation time  $\langle T_2 \rangle$  was calculated as the arithmetic mean of the spectrum. For muscle at 3T,  $\langle T_2 \rangle = 50 \pm 4$  ms. (c) Inversion recovery data for quantitative evaluation of  $T_1$ . Normalized magnetization is shown as a function of inversion recovery time, TI, on a logarithmic timescale. Therefore, the decay curve appears sigmoidal. The data points represent experimental data, whereas the solid line is the fitted curve obtained by using a monoexponential equation  $T_1$  decay model. For muscle at 3 T,  $T_1 = 1412 \pm 13$  ms. (d) Quantitative MT data for a muscle sample. The normalized liquid pool magnetization ( $M_z/M_0$ ) is shown as a function of saturation pulse offset frequency,  $\Delta$ , for 7 applied saturation pulse amplitudes,  $\omega_1/2\pi$ . The solid lines represent a global, 2-pool model fit to the experimental data (points).

ters generated by the same SMIS console. The sole exception involved the specifics of tuned RF coils.

The MR measurements consisted of the following:

- $T_2$  relaxation data acquired using a CPMG sequence (10,11) with TE/TR = 1/15,000 ms, 6000 even echoes sampled, 24 averages, and a DC phase cycling scheme.
- $T_1$  relaxation time data acquired using an inversion recovery (IR) sequence (10) with 35 TI values logarithmically spaced from 1 to 32,000 ms, 20s between each acquisition and the next inversion pulse (TR), and 2 averages.
- Magnetization Transfer (MT) was measured using a continuous-wave (cw) saturation pulse of 7 s duration. To evaluate MT data (12) quantitatively, 7 RF saturation amplitudes ( $\omega_1/2\pi = 85, 170, 340, 670, 1340, 2670, \text{ and } 5340$  Hz) and 26 off-resonance frequencies,  $\Delta$  (logarithmically spaced from 0.014 to 250 kHz), were applied. The repetition time, TR, was 20s, and the number of averages was 4. For the “standard” magnetization transfer ratio (MTR) evaluation, the RF saturation pulse amplitude,  $\omega_1/2\pi$ , was 670 Hz, and the offset frequency of the saturation,  $\Delta$ , was 5 kHz. The effects of any residual transverse magnetization following the off-resonance irradiation were removed by phase-cycling the  $\pi/2$  pulse ( $-x/x$ ).

To probe  $T_2$  relaxation anisotropy in cartilage, the only tissue in this study to show this effect (13), the  $T_2$  relaxation experiments were performed for 2 angular orientations in respect to the major collagen fibers:  $0^\circ$  and the

magic angle of  $55^\circ$  (13). MR properties of blood were measured at a blood oxygen level of 95%. Diffusion properties were not measured because it has been shown previously that the Brownian motion of water molecules does not depend on the external magnetic field strength (14,15).

#### Data Analysis

Illustrative  $T_2$  data for muscle tissue are presented in Fig. 1a. All  $T_2$  decay data were fitted to a multi-component  $T_2$  model by using a Non-Negative Least-Squares (NNLS) algorithm resulting in a fitted  $T_2$  spectrum (16), presented in Fig. 1b. The  $T_2$  spectrum shows the relative signal amplitude per logarithmic interval as a function of  $T_2$  relaxation. As a single-parameter summary of these  $T_2$  spectra, an average  $T_2$  relaxation time,  $\langle T_2 \rangle$ , was calculated as the arithmetic mean of the  $T_2$  spectrum (Fig. 1b).  $\langle T_2 \rangle$  is similar to the mono-exponential estimate of  $T_2$  decay that is usually assessed in clinical MR except it is estimated with much shorter echo times (TE = 1ms) and it is measured above (beyond) 1 s, a region that is not usually evaluated in clinical imaging.

The  $T_1$  data were analyzed assuming mono-exponential behavior. This assumption is valid for all the measured tissues, because on the time scale of  $T_1$  measurement (typically a couple of seconds) the inter-compartmental exchange achieves total mixing of intra- and extra-cellular pools (17,18) and mono-exponential relaxation recovery is anticipated (19). An example of inversion recovery data for muscle tissue is presented in Fig. 1c. The abscissa is the

Table 1  
 $T_2$  and  $T_1$  Relaxation Times at 3T and 1.5T Measured at 37°C. Literature data is also shown.

Tissue	$T_2$ —3 T [ms]		$T_1$ —3 T [ms]		$T_2$ —1.5 T [ms]		$T_1$ —1.5 T [ms]	
	This study	Literature	This study	Literature	This study	Literature	This study	Literature
Liver	42 ± 3		812 ± 64		46 ± 6	54 ± 8 <sup>(35)</sup>	576 ± 30	~600 <sup>(23)</sup>
Skeletal muscle	50 ± 4	32 ± 2 <sup>(25)</sup>	1412 ± 13	1420 ± 38 <sup>(25)</sup>	44 ± 6	35 ± 4 <sup>(25)</sup>	1008 ± 20	1060 ± 155 <sup>(25)</sup>
Heart	47 ± 11		1471 ± 31		40 ± 6	44 ± 6 <sup>(36)</sup>	1030 ± 34	
Kidney	56 ± 4		1194 ± 27		55 ± 3	61 ± 11 <sup>(37)</sup>	690 ± 30	709 ± 60 <sup>(37)</sup>
Cartilage 0°	27 ± 3	37 ± 4 <sup>(25)</sup>	1168 ± 18	~1240 <sup>(25)</sup>	30 ± 4	42 ± 7 <sup>(25)</sup>	1024 ± 70	~1060 <sup>(25)</sup>
Cartilage 55°	43 ± 2	45 ± 6 <sup>(26)</sup>	1156 ± 10		44 ± 5		1038 ± 67	
White matter	69 ± 3	56 ± 4 <sup>(27)</sup>	1084 ± 45	1110 ± 45 <sup>(29)</sup>	72 ± 4	79 ± 8 <sup>(38)</sup>	884 ± 50	778 ± 84 <sup>(38)</sup>
Gray matter	99 ± 7	71 ± 10 <sup>(27)</sup>	1820 ± 114	1470 ± 50 <sup>(29)</sup>	95 ± 8	~95 <sup>(39)</sup>	1124 ± 50	1086 ± 228 <sup>(38)</sup>
Optic nerve	78 ± 5		1083 ± 39		77 ± 9		815 ± 30	
Spinal cord	78 ± 2		993 ± 47		74 ± 6		745 ± 37	
Blood	275 ± 50		1932 ± 85	~1550 <sup>(30)</sup>	290 ± 30	327 ± 40 <sup>(14)</sup>	1441 ± 120	~1200 <sup>(30)</sup>

inversion recovery time, TI, on a logarithmic scale. Therefore, the  $T_1$  recovery appears as a sigmoidal curve. The solid line in Fig. 1c represents the mono-exponential fit to the experimental data.

Quantitative MT data were fitted to a “2-pool” model (12,20) quantifying the exchange between an unrestricted (liquid) and a semisolid (macromolecular) pool of restricted mobility. The model estimates: R, the rate of MT exchange of longitudinal magnetization between liquid and semisolid pools,  $M_{OB}$ , the fraction of magnetization that resides in the semisolid pool and undergoes MT exchange, and  $T_{2B}$ , the transverse relaxation time value of the macromolecular protons. For solid tissues, MT data were fitted with a super-Lorentzian lineshape (20), where the width of the macromolecular line-shape was characterized by an estimate of the transverse relaxation time for semisolid pool,  $T_{2B}$ . For blood, a Lorentzian line-shape was used, based on previous observations (21). The magnetization transfer ratio (MTR) was evaluated by the following equation:

$$MTR = (M_0 - M_{SAT})/M_0 \quad [1]$$

where  $M_0$  and  $M_{SAT}$  denote signal amplitude measured without and with the RF saturation pulse, respectively.  $M_{SAT}$  was measured at the RF saturation pulse amplitude

$\omega_1/2\pi = 670$  Hz, and the offset frequency of the RF saturation  $\Delta = 5$  kHz. Fig. 1d shows fitted MT, Z spectra (22), and the measured MT data, enabling more quantitative analysis. Residual, longitudinal magnetization following an RF saturation pulse normalized to magnetization without saturation is plotted as a function of offset frequency,  $\Delta$ , for 7 different RF pulse amplitudes,  $\omega_1/2\pi$ .

## RESULTS

The MR parameters at 37°C and 3 T for the variety of measured tissues are presented in Tables 1 and 2. Table 1 shows 3 and 1.5 T longitudinal,  $T_1$ , and transverse,  $T_2$ , relaxation times and compares those with values obtained from the literature. There was no significant, statistical difference (within the experimental error) between the  $T_2$  relaxation time values at 3 T and 1.5 T.  $T_1$  relaxation time constants for all measured tissues were longer than those at 1.5 T. The percentage increase in  $T_1$  values was not uniform across all measured tissues; it was the largest for kidney (~73%) and smallest for cartilage (~10%). White matter  $T_1$  relaxation time increased by approximately 22%.  $T_1$  increase in blood was approximately 34%; it was 41% for liver, 43% for heart, 40% for skeletal muscle, 62% for gray matter, and 33% for spinal cord and optic nerve.

Quantitative MT parameters at 3 T, as reported in Table 2, also varied among measured tissues. The semisolid

Table 2  
Magnetization Transfer Parameters at 3 T Compared to Literature Data at 1.5 T.

Tissue	This paper measured at 3 T				Literature at 1.5 T		
	$M_{OB}$ [%]	R [s <sup>-1</sup> ]	$T_{2B}$ [μs]	MTR [%]	$M_{OB}$ [%]	R [s <sup>-1</sup> ]	$T_{2B}$ [μs]
Liver	6.9 ± 0.7	51 ± 10	7.7 ± 0.2	77 ± 5		53 ± 6 <sup>(20)</sup>	7.8 ± 0.6 <sup>(20)</sup>
Skeletal muscle	7.4 ± 1.3	66 ± 6	8.7 ± 0.1	88 ± 2	6.9 ± 1.6 <sup>(23)</sup>	70 ± 4 <sup>(23)</sup>	8.2 ± 0.6 <sup>(23)</sup>
Heart	9.7 ± 0.2	52 ± 7	8.1 ± 0.1	89 ± 1	7.2 ± 0.7 <sup>(23)</sup>	57 ± 5 <sup>(23)</sup>	8.4 ± 0.4 <sup>(23)</sup>
Kidney	7.1 ± 1.0	46 ± 7	8.1 ± 0.3	82 ± 1			
Cartilage 0°	17.1 ± 2.4	57 ± 3	8.3 ± 0.1	85 ± 1			
Cartilage 55°	18.2 ± 0.4	60 ± 5	8.3 ± 0.1	86 ± 1			
White matter	13.9 ± 2.8	23 ± 4	10.0 ± 1.0	85 ± 1	15.2 ± 2.3 <sup>(38)</sup>	30 ± 8 <sup>(38)</sup>	11.3 ± 1.8 <sup>(38)</sup>
Gray matter	5.0 ± 0.5	40 ± 1	9.1 ± 0.2	84 ± 1	7.2 ± 1.3 <sup>(38)</sup>	33 ± 9 <sup>(38)</sup>	11.1 ± 1.1 <sup>(38)</sup>
Optic nerve	15.8 ± 1.1	23 ± 2	10.0 ± 0.6	86 ± 2		20 ± 3 <sup>(20)</sup>	10.5 ± 0.5 <sup>(20)</sup>
Spinal cord	12.6 ± 1.8	26 ± 5	10.5 ± 0.6	83 ± 1			
Blood	2.8 ± 0.7	35 ± 7	280 ± 50	11 ± 4	3.3 ± 0.6 <sup>(23)</sup>	40 ± 5 <sup>(23)</sup>	340 ± 40 <sup>(23)</sup>

MTR is measured at the RF saturation pulse amplitude,  $\omega_1/2\pi = 670$  Hz, and the offset frequency of the saturation,  $\Delta = 5$  kHz (optimum MT experimental parameters to achieve maximum MT effect for most of the tissues).

(macromolecular) pool fraction,  $M_{OB}$ , was high for optic nerve ( $15.8 \pm 1.1\%$ ), spinal cord ( $12.6 \pm 1.8\%$ ), and white matter ( $13.9 \pm 2.8\%$ ) and was the largest for cartilage ( $17.1 \pm 2.4\%$ ), whereas it was relatively smaller for muscle ( $7.4 \pm 1.3\%$ ), liver ( $6.9 \pm 0.7\%$ ), heart ( $9.7 \pm 0.2\%$ ), kidney ( $7.1 \pm 1.0\%$ ), gray matter ( $5.0 \pm 0.5\%$ ), and blood ( $2.8 \pm 0.7\%$ ). The MT exchange rate,  $R$ , also varied in the measured samples, ranging from approximately  $25 \text{ s}^{-1}$  for tissues containing white matter (WM, optic nerve and spinal cord) to approximately  $46$  to  $66 \text{ s}^{-1}$  for kidney, heart, liver, cartilage, gray matter, and skeletal muscle. The macromolecular pool  $T_2$  relaxation time,  $T_{2B}$ , was similar for all measured tissues, ranging from  $\sim 7.7 \mu\text{s}$  for liver to  $\sim 10.5 \mu\text{s}$  for spinal cord. Consistent with the literature (20,21,23), blood exhibited a lower MT effect ( $MTR = 11 \pm 4\%$ ) and a different macromolecular pool  $T_2$  relaxation time,  $T_{2B}$  ( $280 \pm 50 \mu\text{s}$ ). Although the MTR values were significantly different among tissues, their range ( $77 \pm 5\%$  for liver and  $89 \pm 2\%$  for heart) was remarkably narrow. The quantitative MT parameters measured at  $1.5 \text{ T}$  were similar to those at  $3 \text{ T}$ .

## DISCUSSION

The major goal of this study was to provide a comprehensive summary of MR parameters at  $3 \text{ T}$ .  $T_2$  relaxation time was found to be independent of magnetic field (Table 1), which is consistent with early observations by Bottomley and coworkers (24). The measured values at  $3$  and  $1.5 \text{ T}$  showed no significant differences within experimental error. Although  $T_2$ -weighted imaging at  $3 \text{ T}$  is quite common, quantitative assessment of  $T_2$  is surprisingly limited. There are (at least to our knowledge) no quantitative  $T_2$  data for liver, heart, kidney, and blood at  $3 \text{ T}$ . The only studies that present quantitative  $T_2$  relaxation times at  $3 \text{ T}$  were performed by Gold and colleagues (25) for cartilage and muscle, Smith and coworkers (26) for cartilage, and Gelman et al. for brain (27).

$T_2$  values obtained by Gold (25) for skeletal muscle and cartilage are significantly lower than the ones obtained in this study. These differences are likely due to differences in pulse sequence techniques. We used a CPMG sequence with a very short echo time (1ms). This relatively short echo time was chosen to minimize the effects of the background gradients (for long TEs) while avoiding the "spin-lock effect" that is typically present at very short echo times (28). Gold's study used much longer TEs (longer than 10ms) and also shows slight decreases in the  $T_2$  relaxation time in muscle and cartilage going from  $1.5$  to  $3 \text{ T}$ , but these differences were within the variation between different subjects. The  $T_2$  relaxation times in this study are much more similar to those obtained by Smith and colleagues (26). By definition, the transverse relaxation time,  $T_2$ , results from time-dependent variations of the effective magnetic field "seen" by an average proton in the measured system. This classic  $T_2$  characteristic (intrinsic  $T_2$  relaxation time) takes into account rotational and diffusional motion of protons in tissue. It does not, however, include *spatially* varying magnetic fields. In particular, the presence of paramagnetic or supermagnetic (iron) particles or altered tissue susceptibility result in microscopic field variations that may not be easily compensated by spin

echo (or CPMG) sequence. Therefore, measured  $T_2$  relaxation time may depend on the external magnetic field and, more importantly on the echo time, TE. It is not surprising, therefore, to observe some decrease in measured literature  $T_2$  values at sufficiently long echo times.

In the case of tissue devoid of paramagnetic impurities, measured  $T_2$  represents an intrinsic  $T_2$  value. For example, in the case of white matter, the  $T_2$  relaxation spectra do not depend on TE or field strength (data not shown). Moreover, accurate  $T_2$  relaxation time estimation relies on the accuracy of  $180^\circ$  pulses, which is not perfect in typical MR imaging. Finally, the  $T_2$  relaxation in tissues is typically not mono-exponential. Therefore, evaluated, apparent  $T_2$  relaxation time (typically based on 2 TE values) depends on the TE chosen for final analysis (Dr Alex MacKay, private communication). In summary, the quantitative assessment of the  $T_2$  relaxation time should be considered with caution.

As for  $T_1$  relaxation, comprehensive comparison between the results of this study and the literature is also possible. For example, there is excellent agreement between the skeletal muscle  $T_1$  obtained in this study ( $1412 \pm 13\text{ms}$ ) and that measured by Gold ( $1420 \pm 38\text{ms}$ ) (25). Similarly,  $3 \text{ T}$  data for cartilage and white matter are comparable with literature values (Table 1).

$T_1$  for gray matter was measured as  $1820 \pm 114 \text{ ms}$ ; however, the value reported by Ethofer and coworkers (29) is significantly ( $1470 \pm 50 \text{ ms}$ ) lower. Similarly, blood  $T_1$  at  $3 \text{ T}$  was longer ( $1932 \pm 85 \text{ ms}$ ) than the literature value of approximately  $1550 \text{ ms}$  (30). This discrepancy probably results from using different methods of  $T_1$  estimation. In the case of Ethofer and colleagues (29), *in vivo*  $^1\text{H}$  magnetic spectroscopy (MRS) was used. Single-voxel spectroscopy in  $2 \text{ cm} \times 2 \text{ cm} \times 2 \text{ cm}$  volumes of interest was performed for different regions of the brain. With such a large volume, it is difficult to avoid partial volume effects; therefore, the  $T_1$  reported may also contain contributions from white matter (which has a lower  $T_1$ ). Moreover, the choice of  $TR = 10,000 \text{ ms}$  by Ethofer (29) is much lower than  $6 \times T_1$ ; hence, it does not allow the magnetization to reach equilibrium, which may contribute to underestimation of  $T_1$  relaxation time. The  $3 \text{ T}$ ,  $T_1$  relaxation time evaluated in the present study for blood ( $1932 \pm 85 \text{ ms}$ ) and heart ( $1471 \pm 31 \text{ ms}$ ) were also significantly higher in comparison to those obtained by Noeske and coworkers (31) ( $1550 \pm 85 \text{ ms}$  and  $1115 \pm 10 \text{ ms}$ , respectively). This discrepancy can probably be explained by the fact that the  $T_1$  relaxation evaluation used by Noeske is measured over a very limited range ( $100 \text{ ms}$  to  $800 \text{ ms}$ ) of TI values, resulting in an underestimation of the intrinsic  $T_1$ .

Quantitative MT parameters varied between measured tissues. These differences can be explained by different macromolecular tissue composition. The tissues exhibiting high lipid (white matter, optic nerve, and spinal cord) or high collagen content (cartilage) exhibited large MT macromolecular fraction,  $M_{OB}$  (between  $12.6$  and  $18.2\%$ ). Conversely, the MT exchange constant,  $R$ , was low for neural, WM tissue (from  $23$  to  $26 \text{ s}^{-1}$ ) and was much higher (from  $40$  to  $66 \text{ s}^{-1}$ ) for muscle, liver, heart, kidney, gray matter, and cartilage. It has been shown that the MT effect in white matter is mostly due to the MT exchange between free water and lipids associated with myelin

sheath (32). The different R values between white matter tissue (WM, optic nerve and spinal cord) and musculoskeletal tissue (liver, muscle, heart, kidney, and cartilage) suggest different exchange constants for lipids (myelin) and proteins or collagen (muscle tissue and cartilage). However, with the exception of blood, the semi-quantitative measure of magnetization transfer, MTR, did not exhibit such large differences between the measured tissues, ranging from 77% for liver to 89% for heart (Table 2). This is consistent with the fact that MTR is proportional to  $RM_{OB} * T_1$  (33). The MT parameter,  $RM_{OB}$ , is similar for all the tissues (low R is compensated by high  $M_{OB}$ , and vice versa, with the exception of cartilage, where both R and  $M_{OB}$  are high and the MT effect reaches its maximum).

In this study, we did not measure MT at 1.5 T. It has been previously shown that quantitative magnetization transfer parameters in model systems (agar) are field independent (12). Tissue degradation, past 3 h, did not allow completion of all MR measurements at two different field strengths for the same sample. However, quantitative MT data at 1.5 T were surprisingly abundant in the literature, enabling quantitative comparison. MT parameters at 3 T did not significantly differ from those obtained at 1.5 T (Table 2).

Comparison of the MTR parameter with the MRI literature has always been difficult. This is because the MTR depends mostly on the MT experimental parameters, such as saturation pulse amplitude and offset frequency. MTR is also a combination of true MT and direct saturation of the liquid pool. For a scientific comparison, MTR values were calculated for an RF saturation scheme for the offset frequency,  $\Delta = 5$  kHz. Standard commercial scanners often use lower offset frequency values,  $\Delta$ , in the range of 1–2 kHz, which are optimal for 3D TOF angiography but not so for the MT effect. There is no single value for the offset frequency that is universally accepted or used. Depending on tissue type and RF pulse saturation scheme, the optimal frequency offset for maximizing the MT effect is between 3 and 8 kHz. However, MT data, as presented here, enabled simulations for a range of experimental pulse sequences, showing that the values of MTR at 3 T are expected to be 2 to 10% lower than those at 1.5 T (data not shown). This small difference in MTR is solely due to increases in  $T_1$  relaxation time. This phenomenon has been confirmed by Duvvuri and coworkers (34), who observed an MTR decrease in white matter by approximately 17% between 1.5 and 4 T.

## CONCLUSIONS

Longitudinal  $T_1$  relaxation times increase with the strength of the magnetic field, while  $T_2$  relaxation and quantitative magnetization transfer parameters are comparatively field independent from 1.5 to 3 T. Based on quantitative MT parameters, MTR is expected to change only slightly; its value decreases by approximately 2 to 10%. Collectively, the results of the present study provide a useful reference for optimization of pulse sequence parameters for MRI at 3 T.

## ACKNOWLEDGMENTS

We would like to thank Dr. Garry Gold, Stanford University, for stimulating discussions during the preparation of

this article, and Mr. Norm Konyer and Ms. Sharon Portnoy, Sunnybrook & Women's CHSC, Toronto, for technical assistance.

## REFERENCES

- Odrobina EE, Lam TYJ, Pun TWC, Midha R, Stanisz GJ. MR properties of excised neural tissue following experimentally induced demyelination. *NMR in Biomed* 2005; in press.
- Pun TWC, Odrobina EE, Xu QG, Lam TYJ, Munro CA, Midha R, Stanisz GJ. Histological and magnetic resonance analysis of sciatic nerves in the tellurium model of neuropathy. *Journal of Peripheral Nervous System* 2005;10:38–46.
- Webb S, Munro CA, Midha R, Stanisz GJ. Is multicomponent T-2 a good measure of myelin content in peripheral nerve? *Magn Reson Med* 2003;49:638–645.
- Does MD, Snyder RE. Multiexponential T-2 relaxation in degenerating peripheral nerve. *Magn Reson Med* 1996;32:207–213.
- Stanisz GJ, Webb S, Munro CA, Pun TWC, Midha R. Properties of neural tissue following experimentally induced inflammation. *Magn Reson Med* 2004;51:473–479.
- Polak JF, Vivaldi MT, Schoen FJ. Proton magnetic resonance of early myocardial infarction in rats. *Invest Radiology* 1988;23:438–442.
- Kleine LJ, Mulkern RV, Guttmann CR, Colucci VM, Jolesz FA. In vivo characterization of cytotoxic intracellular edema by multicomponent analysis of transverse magnetization curves. *Radiology* 1995;2:365–372.
- Frey HE, Knispel RR, Kruuv J, Sharp AR, Thompson RT, Pintar MM. Proton spin-spin lattice relaxation studies of nonmalignant tissue of tumorous mice. *J National Cancer Inst* 1972;49:903–906.
- Bernard E, Mohamed B, Yves M, Chambron J. 1H transverse relaxation times at 200Hz in the intact beating, ischemic and reperfused-viable isolated rat heart. *Magn Res Biol Med* 1994;1:77–97.
- Carr H, Purcell E. Effects of diffusion on free precession in nuclear magnetic resonance experiments. *Phys Rev* 1954;94:630–638.
- Meiboom S, Gill S. Modified spin-echo method for measuring nuclear relaxation times. *Rev Sci Instr* 1958;29:688–691.
- Henkelman RM, Huang X, Xiang Q-S, Stanisz GJ, Swanson SD, Bronskill MJ. Quantitative interpretation of magnetization transfer. *Magn Reson Med* 1993;29:759–766.
- Henkelman RM, Stanisz GJ, Kim JK, Bronskill MJ. Anisotropy of NMR properties of tissues. *Magn Reson Med* 1994;32:592–601.
- Stanisz GJ, Li JG, Wright GA, Henkelman RM. Water dynamics in human blood via combined measurements of T2 relaxation and diffusion in the presence of gadolinium. *Magn Reson Med* 1998;39:223–233.
- Li JG, Stanisz GJ, Henkelman RM. Integrated analysis of diffusion and relaxation of water in blood. *Magn Res Med* 1998;40:79–88.
- Whittall KP, MacKay AL. Quantitative interpretation of NMR relaxation data. *J Magn Reson* 1989;95:134.
- Lee JH, Springer CS. Effects of equilibrium exchange on diffusion-weighted NMR signals: The diffusigraphic "shutter-speed." *Magn Reson Med* 2003;49:450–466.
- Labadie C, Lee JH, Vetek G, Springer CS. Relaxographic imaging. *J Magn Reson Imag* 1994;105:99–112.
- Stanisz GJ. Diffusion MR in biological systems: tissue compartments and exchange. *Israel J Chem* 2003;43:33–44.
- Morrison C, Stanisz GJ, Henkelman RM. Modeling magnetization transfer for biological-like systems using a semi-solid pool with a super-Lorentzian lineshape and dipolar reservoir. *J Magn Reson B* 1995;108:103–113.
- Li JG, Graham SJ, Henkelman RM. A flexible magnetization transfer line shape derived from tissue experimental data. *Magn Reson Imag* 1997;37:866–871.
- Grad J, Bryant RG. Nuclear magnetic cross-relaxation spectroscopy. *J Magn Reson* 1990;90:1–8.
- Graham SJ, Stanisz GJ, Kecojevic A, Bronskill MJ, Henkelman RM. Analysis of changes in MR properties of tissues after heat treatment. *Magn Reson Med* 1999;42:1061–1071.
- Bottomley PA, Foster TH, Argersinger RE, Pfeifer LM. A review of normal tissue hydrogen NMR relaxation times and relaxation mechanisms from 1–100 MHz: dependence on tissue type, NMR frequency, temperature, species, excision, and age. *Med Phys* 1984;11:1184–1197.
- Gold GE, Han E, Stainsby J, Wright GA, Brittain J, Beaulieu C. Musculoskeletal MRI at 3.0T: relaxation times and image contrast. *Am J Neuroradiol* 2004;183:343–350.

26. Smith HE, Mosher TJ, Dardzinski BJ, Collins BG, Collins CM, Yang QX, Schmithorst VJ, Smith MB. Spatial variation in cartilage T2 of the knee. *J Magn Reson Imag* 2001;14:50–55.
27. Gelman N, Gorell JM, Barker PB, Savage RM, Spickler EM, Windham JP, Knight RA. MR imaging of human brain at 3.0 T: preliminary report on transverse relaxation rates and relation to estimated iron content. *Radiology* 1999;210:759–767.
28. Santyr GE, Henkelman RM, Bronskill MJ. Spin locking for magnetic resonance imaging with application to human breast. *Magn Reson Med* 1989;12:25–37.
29. Ethofer T, Mader I, Seeger U, Helms G, Erb M, Grodd W, Ludolph A, Klose U. Comparison of longitudinal metabolite relaxation times in different regions of the human brain at 1.5 and 3 tesla. *Magn Res Med* 2003;50:1296–1301.
30. Greenman RL, Shirsoky JE, Mulkern RV, Rofsky NM. Double inversion black-blood fast spin-echo imaging of the human heart: a comparison between 1.5T and 3.0T. *J Magn Reson Imag* 2003;17:648–655.
31. Noeske N, Seifert F, Rhein K-H, Rinneberg H. Human cardiac imaging at 3 T using phased array coils. *Magn Res Med* 2000;44:978–982.
32. Stanisz GJ, Kecojevic A, Bronskill MJ, Henkelman RM. Characterizing white matter with magnetization transfer and T2. *Magn Reson Med* 1999;42:1128–1136.
33. Henkelman RM, Stanisz GJ, Graham JS. Magnetization transfer in MRI: a review. *NMR in Biomed* 2001;14:57–64.
34. Duvvuri U, Roberts DA, Leigh JS, Bolinger L. Magnetization transfer imaging of the brain: a quantitative comparison of results obtained at 1.5 and 4.0 T. *J Magn Reson Imag* 1999;10:527–532.
35. Cieszanowski A, Szeszkowski W, Golebiowski M, Bielecki DK, Grodzicki M, Pruszyński B. Discrimination of benign from malignant hepatic lesions based on their T2-relaxation times calculated from moderately T2-weighted turbo SE sequence. *Eur Radiology* 2002;12:2273–2279.
36. Allmann KH, Horch R, Uhl M, Gufler H, Althoefer C, Stark GB, Langer M. MR imaging of the carpal tunnel. *Eur J Radiology* 1997;25:141–145.
37. Aherne T, Tscholakoff D, Finkbeiner W, Sechtem U, Derugin N, Yee E, Higgins CB. Magnetic resonance imaging of cardiac transplants: the evaluation of rejection of cardiac allografts with and without immunosuppression. *Circulation* 1986;74:145–156.
38. Sled JG, Pike GB. Quantitative imaging of magnetization transfer exchange and relaxation properties in vivo using MRI. *Magn Reson Med* 2001;46:923–932.
39. Pell GS, Briellmann RS, Waites AB, Abbott DF, Jackson GD. Voxel-based relaxometry: a new approach for analysis of T2 relaxometry changes in epilepsy. *Neuroimage* 2004;21:707–713.